A Non-Resampling Sequential Monte Carlo Detector for Coded OFDM Systems Based on Periodic Termination of Differential Phase Trellis

Thomas S. John, *Student Member, IEEE*, A. Nallanathan, *Senior Member, IEEE*, and Marc A. Armand, *Member, IEEE*

***Abstract*— Sequential Monte Carlo (SMC) is a group of methods that use Monte Carlo simulation to solve online estimation problems in dynamic systems. SMC methods are traditionally built on the techniques of sequential importance sampling (SIS) and resampling. In this paper, we apply the SMC methodology to the problem of symbol detection in a differentially encoded orthogonal frequency division multiplexing (OFDM) system over a frequency selective fading channel. We first propose the periodical termination of differential phase trellis at predetermined indices. It is seen that accelerated weight degeneracy and impoverished trajectory diversity – problems that are encountered in traditional SMC methods – are mitigated. Using these observations, a novel SMC framework that circumvents resampling is then developed. The effect of varying termination periods on the performance of the non-resampling detector is investigated. We also present results which show that periodic termination helps to retard weight degeneracy. The performance of traditional and non-resampling SMC detectors for a convolutional-coded OFDM system is compared and simulation results suggest that the non-resampling detector performs better than its traditional counterpart. We also consider a low-density parity check (LDPC)-coded OFDM system and simulation results suggest the near bound performance of the proposed non-resampling SMC detector.**

***Index Terms*— Sequential Monte Carlo methods, Orthogonal frequency division multiplexing (OFDM), Iterative receivers, Coded modulation.**

I. INTRODUCTION

ORTHOGONAL frequency division multiplexing (OFDM) [1]- [4] is a potential candidate for multimedia wireless services that require high bit rates over mobile radio channels. In OFDM, the entire channel is divided into many narrow sub-channels that are transmitted in parallel, i.e., a frequency-selective fading channel is converted into several flat-fading channels. This increases the symbol duration and reduces the intersymbol interference (ISI). These features make OFDM an effective technique for combating multipath-fading and for high bit rate transmission over wireless mobile channels.

Considerable research has been devoted to symbol detection in slow, flat-fading channels. One such method is the sequential Monte Carlo (SMC) methodology [5]- [9], which originally emerged in the field of statistics to provide a complete theoretical framework for the usage of Monte Carlo methods in dynamic systems [9]. SMC techniques have since been used in fields such as computer vision, speech recognition, and DNA sequence analysis. SMC has also been valuable in communications [10]- [13] because receivers based on the SMC methodology not only utilize *a priori* symbol probabilities, but also produce *a posteriori* symbol probabilities. This feature allows these detectors to serve as the first-stage of an iterative (turbo) receiver. SMC detectors are traditionally built on the techniques of sequential importance sampling (SIS) and resampling. However, resampling procedures introduce practical and theoretical problems [6] such as (i) impoverishment of diverse trajectories, (ii) loss of statistical independence of trajectories, (iii) increased complexity, and (iv) difficulty in implementing the SMC algorithm in parallel. Although resampling gives rise to the aforementioned problems, it is a vital step since degeneracy in the SIS algorithm is unavoidable, i.e., as the SIS algorithm progresses, it tends to carry more imputed trajectories of low importance weights that do not contribute significantly to the final estimation. This is a waste of computational effort and memory. There has been some research effort to develop methods that mitigate the aforementioned problems, or in some cases, skip the resampling procedure [14] - [16]. These methods, however, can be computationally expensive [16].

In this paper, we present a scheme that allows us to circumvent resampling while avoiding an increase in computational complexity when the SMC methodology is applied to a coded OFDM system. We force the phase trellis of a differentially encoded OFDM system to terminate at predetermined indices. Periodic termination of phase trellis has implications on weight degeneracy and trajectory diversity in the SMC framework and these implications are analyzed. Specifically, for an appropriately chosen period, periodic termination helps to retard weight degeneracy and enhance trajectory diversity. This in turn allows the resampling step present in conventional SMC frameworks to be circumvented. The results of this analysis are then applied to the problem of symbol detection in a coded OFDM system employing differential phase modulation over an unknown frequency-selective multipath-fading channel.

The remainder of the paper is organized as follows. Section II describes a coded OFDM system that employs periodically

Manuscript received August 18, 2004; revised March 28, 2005 and July 25, 2005; accepted August 23, 2005. The editor coordinating the review of this paper and approving it for publication is Prof. Vijay K. Bhargava.

Thomas S. John is with the Department of Electrical Engineering, Stanford University, Stanford, CA 94305 (e-mail: thomassj@stanford.edu).

A. Nallanathan and Marc A. Armand are with the Department of Electrical & Computer Engineering, National University of Singapore, 119260 (e-mail: {elena, eleama}@nus.edu.sg).

Digital Object Identifier 10.1109/TWC.2006.04563.

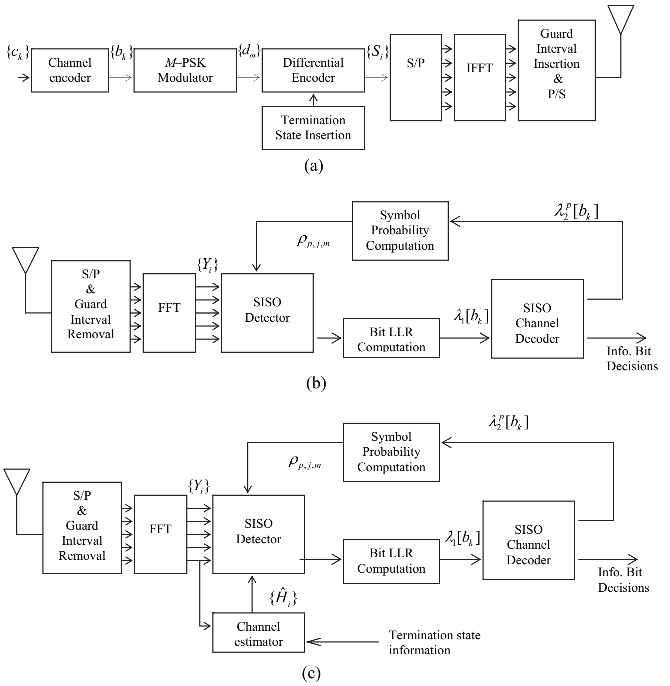

Fig. 1. OFDM system with periodically terminated differential encoder (a) Transmitter (b) Iterative receiver without channel estimator (c) Iterative receiver with channel estimator

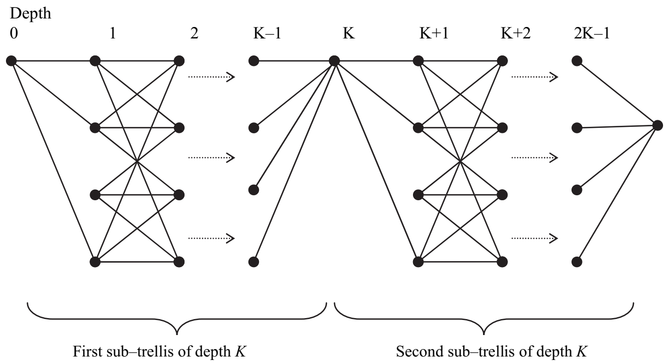

Fig. 2. Phase trellis of differential QPSK with termination period K.

terminated differential phase modulation. The proposed non-resampling SMC detector for coded OFDM systems is introduced in Section III. This detector executes either Algorithm A or Algorithm B. Algorithm A requires pilot-aided channel estimates obtained from an external channel estimator to initialize the detector and estimate *a posteriori* symbol probabilities. Algorithm B, on the other hand, does not require a separate channel estimator for the detector to function. Instead, the detector itself updates the channel statistics using the one-step Kalman filter. Details of these algorithms are provided in Section III. Section IV presents computer simulations that show the validity of our claim that periodic termination retards weight degeneracy. This section also contains results that suggest the promising performance of the proposed non-resampling SMC detector for both convolutional-coded and low-density parity check (LDPC)-coded OFDM systems in various wireless mobile environments.

II. System Model

In this section, we consider a coded OFDM system employing periodically terminated differential phase modulation with single transmit antenna. There are N subcarriers signaling through an unknown frequency-selective multipath-fading channel. It is assumed that the fading process is quasi-static. The transmitted signals are received through a single receive antenna and fed into an iterative receiver after matched filtering and sampling. The transmitter structure used in this paper is shown in Fig. 1(a) and the iterative receiver without and with channel estimator is shown in Fig. 1(b) and Fig. 1(c), respectively. It is convenient to define $[z]$, for all $z \in \mathrm{Z}^+$, as the set containing all non-negative integers less than or equal to z, i.e., $[z] \triangleq \{0, 1, \ldots, z\}$.

A. Baseband Coded OFDM Signal Model

A source produces binary information bits $\{c_k\}$ that are encoded by an outer channel encoder to yield code bits $\{b_k\}$. The bits $\{b_k\}$ are mapped to an M-PSK modulated symbol stream $\{d_\omega\}$ taking values from the finite alphabet, $A_M = \{a_1, a_2, \ldots, a_M\}$. The stream $\{d_\omega\}$ is subsequently fed into a differential encoder that operates at a termination period of$K$, i.e., at every K^{th} transition through the differential M-phase trellis, $\log_2 M$ bits are inserted into the differential encoder to terminate it at the desired state. This terminated state then acts as the initial state for the next $K-1$ data symbols before being terminated once again on the K^{th} transition. This continues until the entire set $\{d_\omega\}$ has been encoded. This periodic termination results in a serial concatenation of sub-trellises, each of depth K (see Fig. 2). For an OFDM system employing N subcarriers, transitions along the phase trellis may then be viewed as symbols transmitted from one subcarrier to the next. Therefore, periodic termination gives rise to a set of N/K subcarriers, $\Omega = \left\{0^{th}, K^{th}, 2K^{th} \ldots, ((N/K)-1)\, K^{th}\right\}$, assuming K divides N. This set Ω is designated to transmit the terminated states. It is clear that a smaller K, i.e., a more frequent termination, will cause the cardinality of Ω to increase and thereby increase overheads. To illustrate, consider $K-1$ M-PSK symbols $\{d_{p,j}\}_{j=1}^{K-1}$ that are differentially encoded to yield the p^{th} sub-trellis, $p \in [(N/K)-1]$:

$$\zeta_{p,j} \triangleq \begin{cases} a_{p,\text{initial}} & ; \ \ j = 0 \\ \zeta_{p,j-1} \cdot d_{p,j}; & j = 1, \ldots, K-1 \end{cases} \tag{1}$$

where $a_{p,\text{initial}} \in A_M$ is the initial state of the p^{th} sub-trellis, or equivalently, the terminated state of the $(p-1)^{th}$ sub-trellis. Thus, for the p^{th} sub-trellis, we obtain the set of symbols $\mathrm{T}_p \triangleq \{\zeta_{p,j}\}_{j \in [K-1]}$. For every OFDM symbol (one time slot), the result is the parallel set of N data and termination symbols:

$$\{S_i\}_{i \in [N-1]} \triangleq \bigcup_{p \in [(N/K)-1]} \mathrm{T}_p \tag{2}$$

The set $\{S_i\}_{i \in [N-1]}$ is then sent through a conventional OFDM transmitter. For an OFDM system with proper cyclic extensions and sample timing with tolerable leakage, the demultiplexed sample Y_i at the i^{th} subcarrier can be expressed as [13]

$$Y_i = S_i H_i + V_i, \quad i \in [N-1] \tag{3}$$

where V_i is the ambient noise which is circularly symmetric complex Gaussian noise with zero mean and variance σ^2, i.e., $V_i \sim \mathrm{N_C}(0, \sigma^2)$. Further, H_i which is the complex channel frequency response at the i^{th} subcarrier, is obtained from the channel's impulse response h by [17]

$$\begin{aligned} H_i &\triangleq H(i\Delta_f) \\ &= \sum_{l=0}^{L-1} \alpha_l \exp\left(-j\frac{2\pi i l}{N}\right) \\ &= h^H w_f(i) \end{aligned} \tag{4}$$

where Δ_f is the tone spacing of the OFDM system, L is the channel length, and $(\cdot)^H$ denotes the Hermitian transpose. The vector $h \triangleq (\alpha_0, \ldots, \alpha_{L-1})^H$ contains the time responses of the resolvable channel taps and $w_f(i) \triangleq \left(1, \ldots, e^{\left(-j\frac{2\pi i(L-1)}{N}\right)}\right)^T$ is the vector containing the FFT coefficients. Substituting (4) into (3) yields

$$Y_i = S_i h^H w_f(i) + V_i, \quad i \in [N-1] \tag{5}$$

Equation (5) shows the explicit relationship among the channel impulse response h, the ambient noise V_i, and the transmitted signal S_i. The demultiplexed samples $\{Y_i\}_{i\in[N-1]}$ are then sent to the iterative receiver. In the following subsection, we describe a generic iterative receiver that processes the set $\{Y_i\}_{i\in[N-1]}$.

B. Iterative Receiver

Since the combination of M-PSK modulation and differential encoding can be viewed as an inner encoder, the aforementioned system is therefore a serial concatenation of two encoders. Generically, a turbo receiver consists of two stages: a soft-input soft-output (SISO) detector followed by a SISO channel decoder.

This SISO detector utilizes the channel estimates, *a priori* symbol probabilities $\rho_{p,j,m} \triangleq \Pr(d_{p,j} = a_m)$, and observation samples $\mathbf{Y} \triangleq \{Y_0, Y_1, \ldots, Y_{N-1}\}$ as inputs to produce *a posteriori* symbol probabilities $\Pr(d_{p,j} = a_m|\mathbf{Y})$ as its output. The channel decoder on the other hand, uses the *a priori* log-likelihood ratios (LLR) of the code bits and delivers an update of the *a posteriori* LLRs of the code bits. Being SISO in nature, the detector and the channel decoder exchange *extrinsic* information with each other to improve the receiver's performance iteratively. Although the *extrinsic* information exchanged are statistically independent at the first iteration, they become progressively more correlated as the iterations proceed. The reader is referred to [18] for details on the computation of the LLRs and *extrinsic* information.

III. Non-Resampling SMC Detector for OFDM Systems

In this section, we present our non-resampling SMC detector for the coded OFDM system described in Section II employing differential$M$-PSK modulation over a frequency-selective multipath-fading channel. Specifically, we look into the problem of estimating the *a posteriori* probabilities of symbols $\{d_{p,j}\}_{j=1}^{K-1}$ for $p \in [(N/K)-1]$ in (1). Before presenting the algorithm, we briefly review the SMC methodology. We also investigate the implications of periodic trellis termination on weight degeneracy and trajectory diversity. We then show how these implications naturally lead to our non-resampling SMC framework.

A. Preliminaries

Consider the state-space model of a discrete dynamic system, i.e.,

$$\begin{aligned} &\text{State equation} &&: \quad z_i = \Theta_i && \text{(6a)} \\ &\text{Observation equation} &&: \quad y_i = \Phi_i(z_i, v_i) && \text{(6b)} \end{aligned}$$

where z_i, y_i, u_i, v_i are the state variable, observation, state noise and observation noise at index i, respectively. Let $Z_i \triangleq (z_0, z_1, \ldots, z_i)$, $Y_i \triangleq (y_0, y_1, \ldots, y_i)$, and suppose an online estimate of some function $\upsilon(Z_i)$ of state variables Z_i is needed, based on observations Y_i. This may be estimated using

$$E\left[\upsilon(Z_i)|Y_i\right] = \int \upsilon(Z_i) f(Z_i|Y_i)\, dZ_i \tag{7}$$

where $f(Z_i|Y_i)$ is the *a posteriori* density of the variables Z_i, given the observations Y_i, and $E[\cdot]$ denotes the expectation operator. Equation (7) requires integrals that are difficult to compute in closed form, but Monte Carlo methods allow us to simplify (7) by sampling from the *a posteriori* density, $f(Z_i|Y_i)$. The estimate of $\upsilon(Z_i)$ is then written as [11]:

$$\hat{E}\left[\upsilon(Z_i)|Y_i\right] = \lim_{\Psi\to\infty} \frac{1}{\Psi} \sum_{q=1}^{\Psi} \upsilon(Z_i^{(q)}) \tag{8}$$

where Ψ is the number of samples used in the estimation of $\upsilon(Z_i)$ and $Z_i^{(q)}$ is the q^{th} random sample drawn from the distribution $f(Z_i|Y_i)$. The convergence of (8) is ensured by the law of large numbers. Direct sampling from the target distribution $f(Z_i|Y_i)$ is often not feasible and hence a trial distribution $g(Z_i|Y_i)$ is sometimes used to generate the set of samples $\left\{Z_i^{(q)}\right\}_{q=1}^{\Psi}$. In importance sampling, the weight $w_i^{(q)}$ is associated with each of the Ψ trajectories in the set $\left\{Z_i^{(q)}\right\}_{q=1}^{\Psi}$, where $w_i^{(q)} = \frac{f(Z_i^{(q)}|\, Y_i)}{g(Z_i^{(q)}|\, Y_i)}$. The pair $\{Z_i^{(q)}, w_i^{(q)}\}_{q=1}^{\Psi}$ is known as a properly weighted sample with respect to the target distribution $f(Z_i|Y_i)$. These properly weighted samples may be used to estimate $E[\upsilon(Z_i)|Y_i]$ by [11]:

$$\hat{E}\left[\upsilon(Z_i)|Y_i\right] = \frac{1}{W_i} \sum_{q=1}^{\Psi} \upsilon(Z_i^{(q)}) w_i^{(q)} \tag{9}$$

where $W_i = \sum_{q=1}^{\Psi} w_i^{(q)}$. The Markov structure of (6a) allows importance sampling to proceed sequentially. The sequential importance sampling (SIS) algorithm used to propagate a set of properly weighted samples from index $i-1$ to index i is described in Table I [11]. As seen in Table I, the choice of trial distribution $g(Z_i|Y_i)$ is important and a useful choice is of the form [9]:

$$\begin{aligned} g(z_i|\, Z_{i-1}^{(q)}, Y_i) &= f(z_i|\, Z_{i-1}^{(q)}, Y_i) \\ &= \frac{f(y_i|\, z_i) f(z_i|\, z_{i-1}^{(q)})}{f(y_i|\, z_{i-1}^{(q)})} \end{aligned} \tag{10}$$

For the trial distribution in (10), the sequential updating of the weight $w_i^{(q)}$ follows [9]:

$$w_i^{(q)} \propto w_{i-1}^{(q)} \cdot f(y_i| \, Z_{i-1}^{(q)}, Y_{i-1}); \quad q = 1, \ldots, \Psi; \quad i \geq 0 \quad (11)$$

where w_{-1} is usually initialized to unity.

TABLE I
A SEQUENTIAL MONTE CARLO ALGORITHM FOR PROPAGATING A SET OF PROPERLY WEIGHTED SAMPLES FROM INDEX $(i-1)$ TO INDEX i

INITIALIZE: Draw a set of independent and identically distributed (i.i.d.) samples $z_{-1}^{(1)}, z_{-1}^{(2)}, \ldots, z_{-1}^{(\Psi)}$ from $f(z_{-1}| \, y_{-1})$. When y_{-1} represents the 'null' information, $f(z_{-1}| \, y_{-1})$ corresponds to the *a priori* distribution of z_{-1}.

FOR $q = 1, \ldots, \Psi$; $i \geq 0$

DO:

(1) Draw a sample $z_i^{(q)}$ from the trial distribution $g(z_i| \, Z_{i-1}^{(q)}, Y_i)$ and let $Z_i^{(q)} = (Z_{i-1}^{(q)}, z_i^{(q)})$

(2) Compute the importance weight recursively:
$w_i^{(q)} = w_{i-1}^{(q)} \cdot \frac{f(Z_i^{(q)}| \, Y_i)}{f(Z_{i-1}^{(q)}| \, Y_{i-1}) \, g(z_i^{(q)}| \, Z_{i-1}^{(q)}, Y_i)}$, where $f(\cdot)$ denotes the target distribution.

END

The weight $w_i^{(q)}$ is a measure of the 'quality' of the imputed sequence (trajectory) $Z_i^{(q)}$. Trajectories with small importance weights are said to be ineffective because large computational effort is devoted to updating them although their contribution to the final estimate is negligible. In general, the SIS algorithm will get more inefficient as index i increases because the discrepancy between the target distribution $f(Z_i|Y_i)$ and trial distribution $g(Z_i|Y_i)$ can only increase with i [10]. This progressive inefficiency is called degeneracy. Therefore, in order to make the SIS procedure effective in practice, it is necessary to resample and conventional SMC methods are built on the techniques of SIS and resampling.

A useful criterion that helps to decide if resampling should be performed during index i is the effective sample size $\bar{\Psi}_i$ at index i. This is approximated as [7]:

$$\bar{\Psi}_i \approx \frac{\Psi}{1 + \Psi \cdot \mathrm{Var}(w_i)} \quad (12)$$

where Ψ is the number of trajectories and $\mathrm{Var}(w_i)$ is the variance of the normalized importance weights w_i of these trajectories at index i. The effective sample size $\bar{\Psi}_i$ is a heuristic measurement of the variation of the weights. When the weights are equal (signifying that all Ψ trajectories are drawn close to the mean of the posterior distribution), $\bar{\Psi}_i$ is at its maximum value of Ψ, while a very small effective sample size suggests that one weight dominates all others. In dynamic resampling, when $\bar{\Psi}_i$ is below a predetermined threshold, it is an indication that degeneracy is chronic and resampling is thus invoked. On the other hand, in deterministic resampling, resampling is carried out at specific values of i, regardless of the effective sample size $\bar{\Psi}_i$. Regardless of the scheme employed, resampling procedures introduce the problems mentioned in Section I.

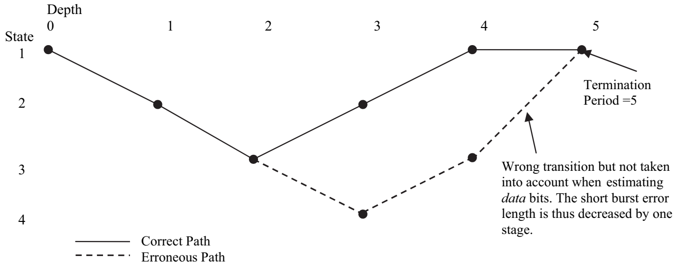

Fig. 3. Possible erroneous path in a sub–trellis.

B. Effect of Periodic Termination on Diversity and Degeneracy in the SMC Framework

The receiver for a system employing differential phase modulation may be designed using conventional SMC methods. This is because (6a) represents the data symbol u_i at index i that causes the transition from phase z_{i-1} to z_i. In (6b), the transmitted symbol z_i is subjected to fading and noise v_i, and observed as y_i. The receiver then has to estimate the correct path through the differential phase trellis $Z_{i,true} \triangleq (z_{0,true}, z_{1,true}, \ldots, z_{i,true})$. Therefore, it is clear that the Ψ properly weighted trajectories $\{Z_i^{(q)}, w_i^{(q)}\}_{q=1}^{\Psi}$ are a collection of possible paths through this trellis and are ideally independent and as diverse as possible. However, the diversity of these Ψ trajectories is reduced when resampling is carried out. Further, the receiver may estimate a path other than the one transmitted, in which case erroneous sequence estimation occurs. Error events along a trellis tend to be bursty and the erroneous path can diverge from and remerge with the correct path any number of times [18]. This bursty nature of error events can lead to accelerated importance weight degeneracy.

Consider differential M-PSK modulation on a set of independent bits in which the total length of transmission of both information symbols and overheads is N, i.e., the trellis consists of N stages. When periodic termination is employed, the phase (state) transition is similar to that shown in Fig. 2 from which interesting observations can be drawn. First, the continuous transmission of information bits is now a series of shorter transmissions corresponding to a serial concatenation of shorter sub-trellises. If the termination period is K, this would give N/K serially concatenated trellises, each of depth K. Thus, each sub-trellis is a transmission window of length K symbols. Second, each sub-trellis is independent of all others, given the initial states. We will exploit these two main effects of periodic termination.

Let us assume that each state is able to transit to M possible states. For a continuous trellis of depth N, there are M^N possible paths through it and N is likely to be of moderate to large length. Even for a system employing binary modulation, i.e., $M = 2$, there will be a significant number of possible paths through the trellis. In the SMC framework, the number of Monte Carlo samples Ψ is of moderate size [7] and it is unlikely these would be able to impute the majority of paths. For example, suppose 9 bits are modulated using differential BPSK. There are 512 possible paths emanating from the initial state. An SMC receiver is required to impute, for example, $\Psi = 50$ samplers. The trajectories imputed by these samplers will, most likely, not be distinct. The effect on the diversity of imputations is clear: The SMC receiver is unlikely to produce many *distinct* trajectories such that sufficient diversity exists after resampling. In fact, to allow for enough diversity to remain after resampling, Ψ would have to be prohibitively large. Now consider a periodically terminated trellis that consists of sub-trellises of depth 5. For binary modulation, each sub-trellis has 32 possible paths and for moderate Ψ, it is likely that there will be more diversity in the imputations.

More distinct trajectories yield more available information and (11) shows how sufficiently diverse trajectories address the issue of degeneracy. The values of each of the Ψ likelihood functions $f(y_i|\ Z_{i-1}^{(q)}, Y_{i-1})$ used in updating the importance weights $w_{i-1}^{(q)}$ will be less degenerated when there are more distinct $\{Z_{i-1}^{(q)}\}_{q=1}^{\Psi}$, i.e., the likelihood functions will occupy a range of values between 0 and 1, inclusive, rather than the extremes of 0 or 1 (which is the case for conventional SMC methods). There are two main reasons for this. First, it is now more likely that there exists at least one correct trajectory among the $\{Z_{i-1}^{(q)}\}_{q=1}^{\Psi}$, and such a trajectory has a large importance weight associated with it. Also, the receiver would have traced a good proportion of erroneous paths, each with an importance weight that is smaller than that corresponding to the correct path. Second, error events along a trellis tend to be bursty, but periodic state termination prevents large burst lengths because (i) erroneous path tracing does not proceed deep into the trellis, and (ii) in the case where the erroneous path remerges with the correct path at the last stage of a sub-trellis, the inserted termination bits are not taken into account in the estimation of data bits and this essentially shortens the erroneous path length by 1 stage (see Fig. 3). The combined result is that degeneracy is retarded while diversity is enhanced. These factors allow the SMC receiver to circumvent the resampling step. Also, the independence of the transmission windows (i) prevents decisions in future indices being affected by a wrong decision made in the current window, and (ii) allows the path estimation through each sub-trellis to be implemented in parallel.

C. Pilot-Aided Non-Resampling SMC Algorithm: Algorithm A

Recall the discrete dynamic system in (6a) and (6b). The corresponding dynamic system that follows from the OFDM system described in Section IIA is:

$$\begin{aligned} &\text{State equation} && : && \zeta_{p,j} = \Theta_{p,j}(\zeta_{p,j-1}, d_{p,j}) && \text{(13a)} \\ &\text{Observation equation} && : && Y_i = \Phi_i(S_i, V_i) && \text{(13b)} \end{aligned}$$

Although the subscripts in (13a) and (13b) are different, we note that $p \in [(N/K)-1]$ and $j \in [K-1]$ are related to the subcarrier index $i \in [N-1]$ through the following

$$i = pK + j \tag{14}$$

Using (14), any set $\{X_i\}_{i\in[N-1]}$ may be represented as $\{X_{pK+j}\}_{p\in[(N/K)-1],\, j\in[K-1]}$ and vice versa.

We apply our non-resampling SMC algorithm to the problem of estimating the *a posteriori* symbol probabilities of $\{d_{p,j}\}_{j=1}^{K-1}$ for $p \in [(N/K)-1]$ based on knowledge of the samples $Y_i \triangleq \{Y_0, \dots Y_i\}$ up to the i^{th} subcarrier, the channel estimates $\{\hat{H}_i\}_{i\in[N-1]}$, henceforth denoted as $\{\hat{H}_{pK+j}\}_{p,j}$, and the *a priori* symbol probabilities of $d_{p,j}$. The set $\{\hat{H}_{pK+j}\}_{p,j}$ may be obtained through pilot-aided channel estimation with the terminated states $\{\zeta_{p,0}\}_{p\in[(N/K)-1]}$ of the differential phase trellis serving as the pilot symbols. Furthermore, the phase of these pilots can be made to cycle through each of the M states $a_1, a_2, \dots, a_M$ in sequence. This method has the advantage of simplicity for both the transmitter and receiver since only the termination period K and the initial state $\zeta_{0,0}$ of the 0^{th} sub-trellis need to be known. To illustrate, consider Ω , the set of N/K subcarriers designated to transmit the terminated states. It is easy to see that the index i of the subcarriers in Ω is related to termination period K through the following:

$$i = (c-1)K, \;\; c = 1, 2, \dots, N/K, \;\; i \in \Omega \tag{15}$$

If the initial state $\zeta_{0,0}$ of the 0^{th} sub-trellis is $a_m \in A_M$, then the phase of the symbol for each $i \in \Omega$ must follow:

$$S_{(c-1)K} = \begin{cases} a_{(m-1+c) \bmod M} & ; \;\; m-1+c \neq 0 \bmod M \\ a_M & ; \;\; m-1+c = 0 \bmod M \end{cases} \tag{16}$$

where $c = 1, 2, \dots, N/K$. Equations (15) and (16) show that the phase of the terminated states are easily obtained from knowledge of $\zeta_{0,0}$, N, K and M.

Another issue of interest is the arrangement of pilots from one OFDM symbol (time slot) to the next. A possible method to make the set of pilot subcarriers at the $(t-1)^{th}$ time slot different from that in the t^{th} time slot is to vary the termination period K from one time slot to the next, in a predetermined fashion. The channel is then estimated using the two-dimensional minimum mean square error (MMSE) interpolation scheme of [20] that employs Wiener filtering.

When the receiver knows the channel estimate $\hat{H}_{pK+j}$, the predictive distribution of the states is given by $\Pr\left(S_{pK+j}|S_{pK+j-1}^{(q)}, Y_{pK+j}, \hat{H}_{pK+j}\right)$, where $S_{pK+j-1}^{(q)}$ is the q^{th} imputed trajectory up to the $(pK+j-1)^{th}$subcarrier, i.e., $S_{pK+j-1}^{(q)} \triangleq \left(S_0^{(q)}, S_1^{(q)}, \dots, S_{pK+j-1}^{(q)}\right)$. It follows that the importance weights are then updated according to:

$$w_{pK+j}^{(q)} \propto w_{pK+j-1}^{(q)} \cdot f\left(Y_{pK+j}|S_{pK+j-1}^{(q)}, Y_{pK+j-1}, \hat{H}_{pK+j}\right) \tag{17}$$

To obtain $f\left(Y_{pK+j}|S_{pK+j-1}^{(q)}, Y_{pK+j-1}, \hat{H}_{pK+j}\right)$ in (17), we first note that the term

$$f\left(Y_{pK+j}|S_{pK+j-1}^{(q)}, Y_{pK+j-1}, \hat{H}_{pK+j}, S_{pK+j} = a_m\right)$$

is a Gaussian likelihood function with mean $\mu_{p,j,m}^{(q)}$ and variance $\sigma_{p,j,m}^{2(q)}$, given by:

$$\begin{aligned} \mu_{p,j,m}^{(q)} &\triangleq E\left[Y_{pK+j}|S_{pK+j-1}^{(q)}, Y_{pK+j-1}, \hat{H}_{pK+j}, S_{pK+j} = a_m\right] \\ &= a_m \hat{H}_{pK+j} \end{aligned} \tag{18}$$

$$\begin{aligned} \sigma_{p,j,m}^{2(q)} &\triangleq \mathrm{Var}\left[Y_{pK+j}|S_{pK+j-1}^{(q)}, Y_{pK+j-1}, \hat{H}_{pK+j}, S_{pK+j} = a_m\right] \\ &= \sigma^2 \end{aligned} \tag{19}$$

where σ^2 is the variance of V_{pK+j} as previously defined. The function of interest, $f\left(Y_{pK+j}|S^{(q)}_{pK+j-1}, Y_{pK+j-1}, \hat{H}_{pK+j}\right)$, can then be obtained from $f\left(Y_{pK+j}|S^{(q)}_{pK+j-1}, Y_{pK+j-1}, \hat{H}_{pK+j}, S_{pK+j} = a_m\right)$ using

$$f\left(Y_{pK+j}|S^{(q)}_{pK+j-1}, Y_{pK+j-1}, \hat{H}_{pK+j}\right) = \sum_{a_m \in A_M} \underbrace{\begin{Bmatrix} f\left(Y_{pK+j}|S^{(q)}_{pK+j-1}, Y_{pK+j-1}, \hat{H}_{pK+j}, S_{pK+j} = a_m\right) \\ \cdot \Pr\left(S_{pK+j} = a_m|S^{(q)}_{pK+j-1}, Y_{pK+j-1}, \hat{H}_{pK+j}\right) \end{Bmatrix}}_{\triangleq \alpha^{(q)}_{p,j,m}} \tag{20}$$

The second term on the right hand side of (20) is the *a priori* probability of symbol $d_{p,j}$ since S_{pK+j} is independent of Y_{pK+j-1} and $\hat{H}_{pK+j}$, and $\{S_{pK+j}\}_{p,j}$ is a Markov chain. The weight update in (17) follows from (20), i.e.,

$$w^{(q)}_{pK+j} \propto w^{(q)}_{pK+j-1} \cdot \sum_{a_m \in A_M} \alpha^{(q)}_{p,j,m} \quad . \tag{21}$$

Furthermore, $\alpha^{(q)}_{p,j,m}$, defined in (20), is proportional to the state predictive distribution via the relation:

$$\begin{aligned} &\Pr\left(S_{pK+j} = a_m|S^{(q)}_{pK+j-1}, Y_{pK+j}, \hat{H}_{pK+j}\right) \\ &= \frac{\begin{bmatrix} f\left(Y_{pK+j}|S^{(q)}_{pK+j-1}, Y_{pK+j-1}, \hat{H}_{pK+j}, S_{pK+j} = a_m\right) \\ \cdot \Pr\left(S_{pK+j} = a_m|S^{(q)}_{pK+j-1}, Y_{pK+j-1}, \hat{H}_{pK+j}\right) \end{bmatrix}}{f(Y_{pK+j}|S^{(q)}_{pK+j-1}, Y_{pK+j-1}, \hat{H}_{pK+j})} \\ &= \frac{\alpha^{(q)}_{p,j,m}}{\sum_{a_m \in A_M} \alpha^{(q)}_{p,j,m}} \propto \alpha^{(q)}_{p,j,m}, \ \forall a_m \in A_M \cdot \end{aligned} \tag{22}$$

With the weight update and state predictive distribution accounted for in (21) and (22), respectively, the pilot-aided non-resampling SMC algorithm proceeds as outlined in Table II.

The estimate of the *a posteriori* probability of symbol $d_{p,j}$ is then made in the p^{th} estimation window for each $p \in [(N/K) - 1]$ according to:

$$\begin{aligned} &\Pr\left(d_{p,j} = a_m|Y_{pK+j}\right) = \Pr\left(S_{pK+j}S^*_{pK+j-1} = a_m|Y_{pK+j}\right) \\ &= E\left[\mathrm{I}\left(S^{(q)}_{pK+j}S^{(q)*}_{pK+j-1} = a_m\right)|Y_{pK+j}\right] \\ &\approx \frac{1}{W_{pK+j}} \sum_{q=1}^{\Psi} \mathrm{I}\left(S^{(q)}_{pK+j}S^{(q)*}_{pK+j-1} = a_m\right) \cdot w^{(q)}_{pK+j} \end{aligned} \tag{23}$$

where $a_m \in A_M,\ j = 1, \ldots, K-1,\ W_{pK+j} = \sum_{q=1}^{\Psi} w^{(q)}_{pK+j}$ and $\mathrm{I}(\cdot)$ is the indicator function, defined as

$$\mathrm{I}(\mathrm{X} = a) = \begin{cases} 1, & \text{if } \mathrm{X} = a \\ 0, & \text{otherwise.} \end{cases} \tag{24}$$

We note that the algorithm in Table II does not consider the normalization of importance weights $\left\{w^{(q)}_{pK+j}\right\}^{\Psi}_{q=1}$ since any SMC algorithm requires only the relative contribution of each weight $w^{(q)}_{pK+j}$ and normalization factors do not affect the performance of the algorithm [9]. Furthermore, all weights are finally normalized by the factor W_{pK+j} in the estimate of the *a posteriori* probability of symbol $d_{p,j}$ (see (23)). The *a posteriori* probabilities $\{\Pr(d_{p,j} = a_m|Y_{pK+j})\}_{p,j,m}$ are then passed to the SISO channel decoder. Following the desired number of turbo iterations between the decoder and detector, the SISO decoder makes a hard decision on the received symbols. This completes the description of our proposed pilot-aided non-resampling SMC algorithm which we refer to as Algorithm A and summarize in Table II.

TABLE II
A NON–RESAMPLING SMC DETECTOR FOR OFDM SYSTEMS EMPLOYING DIFFERENTIAL M–PSK MODULATION
(ALGORITHM A)

For each pair (p, q) *where* $p \in [(N/K) - 1]$; $q = 1, \ldots, \Psi$,

DO:

0. Initialization: Obtain channel estimates $\hat{H}_{pK+j}, j \in [K-1]$ and initialize all importance weights to $w^{(q)}_{-1} = 1$.

The following steps are implemented at the j^{th} index for each pair (p, q), $j \in [K-1]$:

1. For each $a_m \in A_M$, compute the following using the results in (18)–(20):

$$\begin{aligned} &\Pr(S_{pK+j} = a_m|S^{(q)}_{pK+j-1}, Y_{pK+j}, \hat{H}_{pK+j}) \\ &\propto f(Y_{pK+j}|S^{(q)}_{pK+j-1}, Y_{pK+j-1}, \hat{H}_{pK+j}, S_{pK+j} = a_m) \\ &\qquad \cdot \Pr(S_{pK+j} = a_m|S^{(q)}_{pK+j-1}) \\ &= \underbrace{\frac{1}{\pi\sigma^{2(q)}_{p,j,m}} \exp\left\{-\frac{\|Y_{pK+j} - \mu^{(q)}_{p,j,m}\|^2}{\sigma^{2(q)}_{p,j,m}}\right\} \cdot \Pr(S_{pK+j} = a_m|S^{(q)}_{pK+j-1})}_{\triangleq \alpha^{(q)}_{p,j,m}} \end{aligned}$$

2. Impute the symbol $S^{(q)}_{pK+j} \in A_M$ with probability:

$\Pr(S_{pK+j} = a_m|S^{(q)}_{pK+j-1}, Y_{pK+j}, \hat{H}_{pK+j}) \propto \alpha^{(q)}_{p,j,m}$

3. Compute the importance weight recursively:

$w^{(q)}_{pK+j} = w^{(q)}_{pK+j-1} \cdot \sum_{a_m \in A_M} \alpha^{(q)}_{p,j,m}$

4. IF $j = K - 1\ \forall(p, q)$ STOP. ELSE return to 1.

END

Unlike conventional SMC methods, Algorithm A does not resample at any subcarrier. Instead, we allow SIS to proceed for all Ψ samplers, and for the N/K sub-trellises of each sampler. This is because the termination states help to retard degeneracy and enhance trajectory diversity, which in turn allows us to circumvent resampling. This significantly reduces the complexity of the proposed non-resampling SMC algorithm. This non-resampling framework also allows us to parallelize computations greatly, since (i) the Ψ samplers are strictly independent now that resampling is not invoked, and (ii) when termination states are known, which is the case with pilot-aided channel estimation, all sub-trellises in the q^{th} sampler are independent. The combined effect is that the p^{th} sub-trellis of the q^{th} trajectory is independent of all others.

A disadvantage of the preceding algorithm is its reliance on an external channel estimator. This is because the algorithm requires channel estimates $\{\widehat{H}_{pK+j}\}_{p,j}$ in all its necessary computations in (18) to (22). Since accurate channel estimates yield more reliable imputations $\left\{S^{(q)}_{pK+j}\right\}^{\Psi}_{q=1}$, and vice versa, the algorithm's performance depends on the quality of the set $\{\widehat{H}_{pK+j}\}_{p,j}$ used in initialization. Furthermore, the receiver's overall complexity is increased by the channel estimator. To overcome these disadvantages, we introduce in the next subsection, a non-resampling SMC detector that allows us to estimate the *a posteriori* symbol probabilities of $d_{p,j}$ as well as the *a posteriori* mean and covariance of the channel. We refer to this alternative approach as Algorithm B. The motivation for further employing periodic termination is that it allows us to skip resampling, thus yielding a low-complexity detector that is independent of other receiver components.

D. Non-Resampling SMC Algorithm without Pilot-Aided Channel Estimation: Algorithm B

We first assume that the channel impulse response h, of length L, has an *a priori* Gaussian distribution with mean vector ε_{-1} and covariance matrix Σ_{-1}. Following (10), the sample for subcarrier $pK+j$ is drawn from the distribution $\Pr\left(S_{pK+j}|S_{pK+j-1}^{(q)}, Y_{pK+j}\right)$, and consequently the importance weights are updated according to:

$$w_{pK+j}^{(q)} \propto w_{pK+j-1}^{(q)} \cdot f\left(Y_{pK+j}|S_{pK+j-1}^{(q)}, Y_{pK+j-1}\right). \tag{25}$$

To obtain $f\left(Y_{pK+j}|S_{pK+j-1}^{(q)}, Y_{pK+j-1}\right)$, we first note the following:

$$\begin{aligned} & f\left(Y_{pK+j}|S_{pK+j-1}^{(q)}, Y_{pK+j-1}\right) \\ & \propto \sum_{a_m \in A_M} \begin{array}{l} f\left(Y_{pK+j}|S_{pK+j-1}^{(q)}, Y_{pK+j-1}, S_{pK+j}=a_m\right) \\ \cdot \Pr\left(S_{pK+j}=a_m|S_{pK+j-1}^{(q)}, Y_{pK+j-1}\right) \end{array} \\ & = \sum_{a_m \in A_M} \underbrace{\begin{Bmatrix} f\left(Y_{pK+j}|S_{pK+j-1}^{(q)}, Y_{pK+j-1}, S_{pK+j}=a_m\right) \\ \cdot \Pr\left(S_{pK+j}=a_m|S_{pK+j-1}^{(q)}\right) \end{Bmatrix}}_{\triangleq\, \alpha_{p,j,m}^{(q)}} \end{aligned} \tag{26}$$

The term $f\left(Y_{pK+j}|S_{pK+j-1}^{(q)}, Y_{pK+j-1}, S_{pK+j}=a_m\right)$ in (26) is Gaussian since it can be written as an integral of a Gaussian density with respect to another Gaussian density [13]:

$$\begin{aligned} & f\left(Y_{pK+j}|S_{pK+j-1}^{(q)}, Y_{pK+j-1}, S_{pK+j}=a_m\right) \\ & = \int f\left(Y_{pK+j}|S_{pK+j-1}^{(q)}, Y_{pK+j-1}, S_{pK+j}=a_m, h\right) \cdot \\ & \qquad f\left(h|S_{pK+j-1}^{(q)}, Y_{pK+j-1}\right) dh \end{aligned} \tag{27}$$

The mean $\mu_{p,j,m}^{(q)}$ and variance $\sigma_{p,j,m}^{2(q)}$ of $f\left(Y_{pK+j}|S_{pK+j-1}^{(q)}, Y_{pK+j-1}, S_{pK+j}=a_m\right)$ are given by

$$\begin{aligned} \mu_{p,j,m}^{(q)} & \triangleq E\left[Y_{pK+j}|S_{pK+j-1}^{(q)}, Y_{pK+j-1}, S_{pK+j}=a_m\right] \\ & = a_m w_f^H(pK+j)\varepsilon_{pK+j-1}^{(q)} \end{aligned} \tag{28}$$

$$\begin{aligned} \sigma_{p,j,m}^{2(q)} & \triangleq \mathrm{Var}\left[Y_{pK+j}|S_{pK+j-1}^{(q)}, Y_{pK+j-1}, S_{pK+j}=a_m\right] \\ & = \sigma^2 + w_f^H(pK+j)\Sigma_{pK+j-1}^{(q)} w_f(pK+j) \end{aligned} \tag{29}$$

where $w_f(i) \triangleq \left(1, e^{\left(-j\frac{2\pi i}{N}\right)}, \ldots, e^{\left(-j\frac{2\pi i(L-1)}{N}\right)}\right)^H$. For subcarrier $pK+j$, (28) and (29) make use of the channel's most recent mean ε_{pK+j-1} and covariance Σ_{pK+j-1} instead of $\{\hat{H}_{pK+j}\}_{p,j}$ in (18) and (19). These most recent estimates are obtained from the preceding subcarrier. Using a similar approach as (22), it is easy to see that $\alpha_{p,j,m}^{(q)}$, defined in (26), is proportional to the state predictive distribution $\Pr\left(S_{pK+j}|S_{pK+j-1}^{(q)}, Y_{pK+j}\right)$, i.e., $\Pr\left(S_{pK+j}=a_m|S_{pK+j-1}^{(q)}, Y_{pK+j}\right) \propto \alpha_{p,j,m}^{(q)}$.

We now make use of the one-step Kalman filter to update the *a posteriori* mean and covariance of the channel. Assume that in the q^{th} trajectory, the imputation for subcarrier $pK+j$ is $a_{imputed}$, i.e., $S_{pK+j}^{(q)} = a_{imputed}$. We then update the channel mean $\varepsilon_{pK+j}^{(q)}$ and covariance $\Sigma_{pK+j}^{(q)}$ using

$$\varepsilon_{pK+j}^{(q)} = \varepsilon_{pK+j-1}^{(q)} + \frac{Y_{pK+j} - \mu_{p,j,imputed}^{(q)}}{\sigma_{p,j,imputed}^{2(q)}}\chi \tag{30}$$

$$\Sigma_{pK+j}^{(q)} = \Sigma_{pK+j-1}^{(q)} - \frac{1}{\sigma_{p,j,imputed}^{2(q)}}\chi\chi^T \tag{31}$$

where $\chi \triangleq \Sigma_{pK+j-1}^{(q)} w_f(pK+j) a_{imputed}^*$. With the predictive distribution and updating of importance weights and channel statistics accounted for, Algorithm B is ready to proceed according to Table III. We see that (30) and (31) are the dominant computations needed in this algorithm. Even so, each term in these equations is easily obtainable.

As in Algorithm A, the *a posteriori* probability of symbol $d_{p,j}$ is made in the p^{th} estimation window for each $p \in [(N/K)-1]$ using (23). Similarly, the symbol *a posteriori* probabilities are passed to the SISO channel decoder which makes a hard decision on the received symbols following a prescribed number of turbo iterations.

E. Computational Complexity of Algorithm A and Algorithm B

In this subsection, we present a brief comparison of the computational complexity of Algorithms A and B. Specifically, we compute the number of multiplications and imputations needed for each (p,q,j), $p \in [(N/K)-1]$, $j \in [K-1]$, $q = 1, \ldots, \Psi$. The result of this investigation is shown in Table IV. It is seen that for a given channel length L, the number of multiplications in both algorithms are linear with respect to M. In particular, the dependence of Algorithm B on L is a result of the one-step Kalman filter used to update the *a posteriori* mean and covariance of the channel. It follows from Table IV that the total number of multiplications needed for Algorithm A and Algorithm B from start to finish is $3MN\Psi$ and $N\Psi\left\{M\left((L+1)^2+1\right)+4L^2\right\}$, respectively. Further, the total number of imputations needed for both algorithms is $N\Psi$.

IV. Simulation Results

In this section, simulation results are provided to show the performance of the non-resampling SMC detectors for the coded OFDM system described in Section III. These non-resampling SMC detectors, which execute Algorithm A or

TABLE III
A NON–RESAMPLING SMC DETECTOR FOR OFDM SYSTEMS EMPLOYING DIFFERENTIAL M–PSK MODULATION
(ALGORITHM B)

For each pair (p, q) where $p \in [(N/K) - 1]$; $q = 1, \ldots, \Psi$,
DO:

0. Initialization: Draw initial samples of the channel vector from $h \sim \mathrm{N_C}(\varepsilon_{-1}, \Sigma_{-1})$. All importance weights are initialized as $w_{-1}^{(q)} = 1$.
The following steps are implemented at the j^{th} index for each pair (p, q), $j \in [K - 1]$:

1. For each $a_m \in A_M$, compute the following using results in (26)–(29):

$$
\begin{aligned}
&\Pr(S_{pK+j} = a_m | S_{pK+j-1}^{(q)}, Y_{pK+j}) \\
&\propto f(Y_{pK+j} | S_{pK+j-1}^{(q)}, Y_{pK+j-1}, S_{pK+j} = a_m) \\
&\qquad\qquad\qquad \cdot \Pr(S_{pK+j} = a_m | S_{pK+j-1}^{(q)}) \\
&= \underbrace{\frac{1}{\pi\sigma_{p,j,m}^{2(q)}} \exp\left\{ -\frac{\|Y_{pK+j} - \mu_{p,j,m}^{(q)}\|^2}{\sigma_{p,j,m}^{2(q)}} \right\} \cdot \Pr(S_{pK+j} = a_m | S_{pK+j-1}^{(q)})}_{\triangleq\, \alpha_{p,j,m}^{(q)}}
\end{aligned}
$$

2. Impute the symbol $S_{pK+j}^{(q)} \in A_M$ with probability:
$\Pr(S_{pK+j} = a_m | S_{pK+j-1}^{(q)}, Y_{pK+j}, \hat{H}_{pK+j}) \propto \alpha_{p,j,m}^{(q)}$

3. Compute the importance weight recursively:
$w_{pK+j}^{(q)} = w_{pK+j-1}^{(q)} \cdot \sum_{a_m \in A_M} \alpha_{p,j,m}^{(q)}$

4. Update the *a posteriori* mean and covariance of the channel using one–step Kalman filter updates. If $S_{pK+j}^{(q)} = a_{imputed}$:

$$
\varepsilon_{pK+j}^{(q)} = \varepsilon_{pK+j-1}^{(q)} + \frac{Y_{pK+j} - \mu_{p,j,imputed}^{(q)}}{\sigma_{p,j,imputed}^{2(q)}} \chi
$$

$$
\Sigma_{pK+j}^{(q)} = \Sigma_{pK+j-1}^{(q)} - \frac{1}{\sigma_{p,j,imputed}^{2(q)}} \chi\chi^T
$$

$$
\text{where} \qquad \chi \triangleq \Sigma_{pK+j-1}^{(q)} w_f(pK + j) a_{imputed}^*
$$

5. IF $j = K - 1$, $\forall (p, q)$ STOP. ELSE return to 1.

END

TABLE IV
COMPARISON OF COMPUTATIONAL COMPLEXITY OF ALGORITHM A AND ALGORITHM B FOR A GIVEN TRIPLET
(p, q, j)

	Algorithm A	Algorithm B
Number of multiplications per (p, q, j)	$3M$	$M \quad (L+1)^2 + 1 \quad + 4L^2$
Number of imputations per (p, q, j)	1	1

Algorithm B, are denoted as NR-SMC(A) and NR-SMC(B), respectively. The traditional SMC detector that is based on both SIS and resampling is also considered and is represented as T-SMC. Similar to the NR-SMC detectors, the T-SMC detector can employ either pilot-aided estimation or the one-step Kalman filter to obtain channel statistics. The T-SMC detector that uses pilot-aided estimation (respectively, Kalman filter updates) is denoted as T-SMC(A) (respectively, T-SMC(B)). The only difference between the corresponding NR-SMC and T-SMC algorithms lies in the resampling step present in the T-SMC detectors. In the T-SMC(A) detector, this resampling step is invoked between steps 3 and 4 in Table II. The T-SMC(B) detector, on the other hand, carries out resampling between steps 4 and 5 in Table III. Therefore, any difference in performance between T-SMC and NR-SMC may be attributed solely to the resampling step. In this paper, we use the deterministic resampling scheme of [9] at every 5^{th} subcarrier.

We restrict modulation to the case where $M = 4$, i.e., QPSK. A channel bandwidth of 800 kHz is divided into $N =$ 64 sub-channels. To make the tones orthogonal to each other, a symbol duration of $80\mu s$ and an additional $20\mu s$ guard interval is used to provide protection from ISI due to multipath delay spread. This results in a total block length of $100\mu s$ and a sub-channel symbol rate of 10 kbits per second. Channels with uniform (UNI), typical urban (TU) and hilly terrain (HT) delay profiles [17], and a Doppler frequency of 40 Hz are used to represent various mobile environments. It is also assumed that the coefficients of the channel's tap delay line are wide-sense-stationary, narrowband, complex, Gaussian random processes with uncorrelated scattering (WSSUS) [21] of band-limited Doppler power spectral density following Jakes' model [22].

We first analyze the effect of varying termination periods on the performance of our proposed NR-SMC detector. It is intuitive that a more frequent trellis termination may improve performance, at the expense of increased overheads. We consider different termination periods, subject to the constraint that K divides $N = 64$ and overheads should not exceed 25%, i.e., $K \in \{32, 16, 8, 4\}$. We also consider the case when the differential phase trellis is not terminated periodically, i.e., $K = \infty$. This coded OFDM system uses a convolutional outer channel encoder of rate half and constraint length 5 with generators $[23\ \ 35]_8$. The SISO channel decoder is the maximum *a posteriori* (MAP) probability algorithm of [23]. Signals are transmitted through a UNI channel of delay spread $\tau_d = 1.06\mu s$ and channel order $L = 3$; although the latter is assumed unknown to the detector. This detector, employing $\Psi = 50$ Monte Carlo samples at every recursion, is then required to trace five fading coefficients. When $K = \infty$, the channel cannot be estimated using pilots since known symbols are not transmitted at any subcarrier, in which case Algorithm A cannot be applied. Instead, we use Algorithm B for all $K \in \{\infty, 32, 16, 8, 4\}$ so that a fair comparison of performance can be made among different values of K. For each K, we ensure that the user's coded symbols occupy a single OFDM time slot. The result of this investigation is shown in Fig. 4. It is seen that when the NR-SMC(B) detector is used, performance improves as K decreases. We also include the performance of the T-SMC(B) detector for $K \in \{\infty, 8, 4\}$. When $K = \infty$, the NR-SMC(B) detector yields a performance loss of roughly 3.5 dB when compared to its traditional counterpart. This is in contrast to $K = 8$ and $K = 4$ where gains of approximately 0.7 dB and 2 dB are observed, respectively. These results highlight the fact that circumventing resampling is beneficial at some values of K, while detrimental at others. This is because a large K yields a sub-trellis that still has a considerable number of possible paths through it. For $\Psi = 50$, it is unlikely

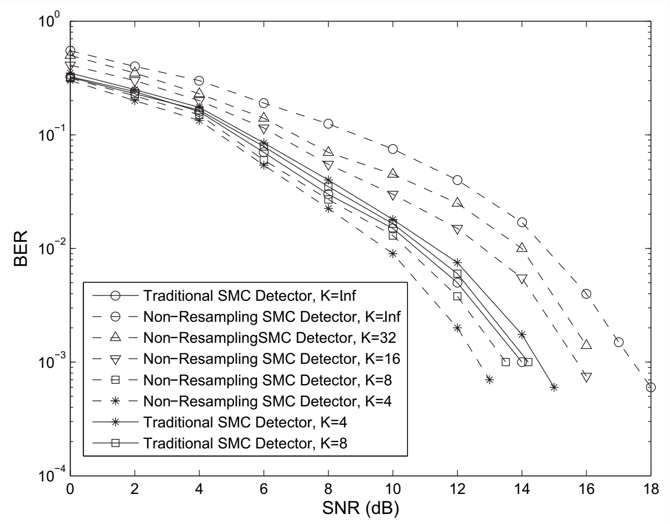

Fig. 4. Effect of varying termination periods on performance of NR–SMC(B) Detector for convolutional–coded OFDM propagated over a UNI channel with $\tau_d = 1.06\mu s$

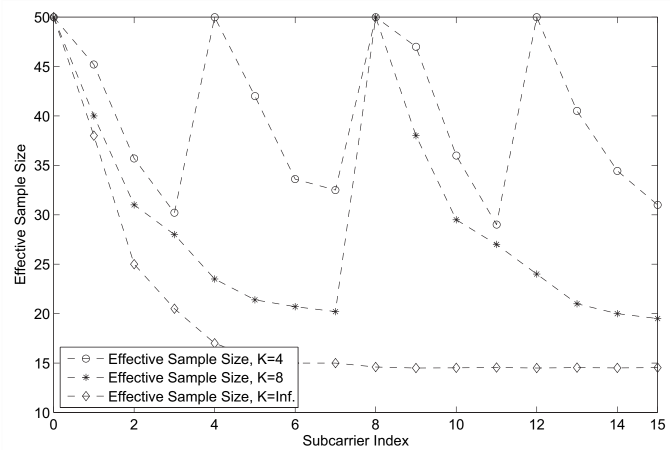

Fig. 5. Effective sample size for first 16 subcarriers of the NR–SMC(B) detector when $K \in \{\infty, 8, 4\}$.

that a good proportion of paths would be traced and this means weight degeneracy still exists. When resampling is circumvented, the inherent degeneracy is not addressed and it therefore propagates quickly from one index to the next, yielding poor estimates. The converse is true for lower values of K.

We also use the preceding system to substantiate the claim that termination states help to retard weight degeneracy. Equation (12), which measures the effective sample size $\bar{\Psi}_i$ at subcarrier i, also provides a convenient way of measuring weight degeneracy. Therefore, we use (12) to calculate $\bar{\Psi}_i$ for the first 16 subcarriers of the NR-SMC(B) detector when $K \in \{\infty, 8, 4\}$. The result of this investigation is shown in Fig. 5. It can be seen that $\bar{\Psi}_i$ drops quickly for $K = \infty$, and is always smaller than $\bar{\Psi}_i$ for any $K \in \{8, 4\}$. Furthermore, the importance weights degenerate the least when $K = 4$ since the effective sample size is greater than any $K \in \{\infty, 8\}$. In addition, the smallest value that $\bar{\Psi}_i$ assumes for $K = 4$ is approximately 60% of the maximum possible value Ψ. These results suggest that more information is available for $K = 4$ since there are more effective samples, and this leads to better performance as seen previously in Fig. 4.

The performance of the traditional and non-resampling SMC frameworks is also compared. We maintain the aforementioned outer channel encoder and set the termination period to $K = 4$, i.e., 25% overheads. As mentioned earlier, the value of K is a tradeoff between performance and overheads. Hence, the exact value chosen is dictated by the particular application. We justify the choice of $K = 4$ by noting that in the OFDM-based IEEE 802.11a standard for wireless local area networks, each OFDM data symbol employs $N = 64$ subcarriers, 52 of which are used for data or pilot symbols. There are also 12 null subcarriers with one in the center and the other 11 on the two ends of the frequency band. Therefore, the IEEE 802.11a standard operates with at least 18.75% overheads regardless of whether pilots are used or not. Since detectors T-SMC(B) and NR-SMC(B) do not have prior knowledge of the channel, the initial mean vector ε_{-1} and covariance matrix Σ_{-1} of h are initialized to an L-by-1 zero vector and $1000I_L$ respectively, where I_L is the L-by-L identity matrix. Note that the large entries in the main diagonal of Σ_{-1} follow from the lack of prior channel knowledge. The required number of turbo iterations between any detector and the MAP decoder is set to 4, and the bit-error-rate (BER) of the information bits is calculated based on observations over a single OFDM symbol duration. The results of this investigation are shown in Fig. 6. It is seen that for $K = 4$, the performance of the NR-SMC(B) detector offers an asymptotic gain of approximately 2 dB over the T-SMC(B) detector. Similarly, the NR-SMC(A) detector offers a gain of approximately 1 dB over the T-SMC(A) detector. Furthermore, the known channel bound, which is obtained by providing perfect channel state information (CSI) to the NR-SMC(A) detector, is approximately 0.5 dB from the asymptotic performance of the NR-SMC(A) detector. These simulation results show that for a fixed algorithm, the NR-SMC detector offers an improvement in performance over the T-SMC detector when $K = 4$. The results also suggest that for a given detector (T-SMC or NR-SMC), Algorithm A performs better than Algorithm B.

An LDPC-coded OFDM system is also investigated. In this paper, the LDPC code is of rate half and encodes a block of 624 information bits. The column weight of the parity check matrix is 3 and the row weights are randomized. Care is taken to ensure that the equivalent factor graph representation of the code has no cycles less than or equal to four. The SISO decoder is the message-passing algorithm [24], which iterates at most 100 times. With termination period K set to 4, the resulting OFDM system is one in which the user's coded symbols occupy 13 consecutive time slots. These symbols are sent through the same UNI channel as in the previous investigation, and a sampling grid spanning five consecutive time slots $t - 2$ to $t + 2$ estimates the channel at time t. The phase of each pilot at any time t is made to cycle through the phases a_1, a_2, a_3 and a_4 in sequence, though K is not varied from one OFDM symbol to the next. Since these pilots are made to estimate the channel as well, the NR-

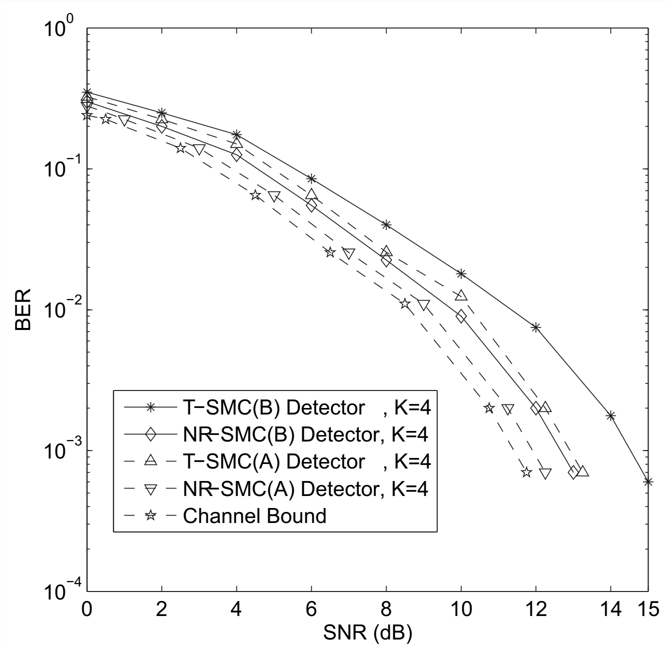

Fig. 6. Comparison of performance between T–SMC and NR–SMC Detectors for convolutional–coded OFDM propagated over a UNI channel with $\tau_d = 1.06\mu s$.

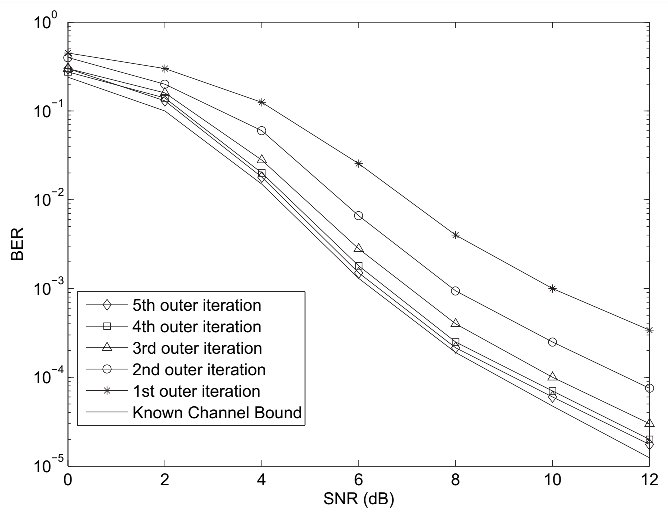

Fig. 7. Effect of number of turbo iterations on performance of NR–SMC(A) detector for LDPC–coded OFDM propagated over a UNI channel with $\tau_d = 1.06\mu s$.

SMC(A) detector is employed. The performance of this system is reflected in Fig. 7. As expected, the gain in performance diminishes with increasing turbo iterations (not to be confused with iterations that occur within the SISO decoder) and 5 turbo iterations yield a performance that is less than 0.5dB from the known UNI channel bound. The effect of other mobile environments on performance is also investigated and in this paper, HT and TU delay profiles of $\tau_d = 5.04\mu s$ and $\tau_d = 1.06\mu s$, respectively, are employed. The number of turbo iterations is maintained at 5 and Fig. 8 shows the performance of the UNI, TU, and HT profiles. It is observed that the delay profiles perform consistently close to their respective channel bounds.

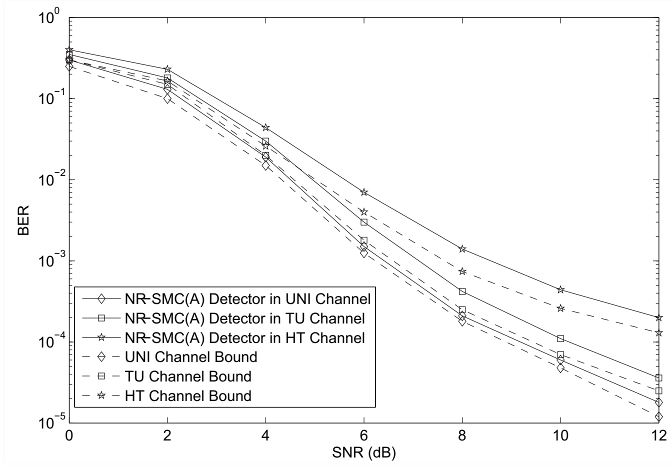

Fig. 8. Performance of NR–SMC(A) detector for LDPC–coded OFDM in HT ($\tau_d = 5.04\mu s$), TU ($\tau_d = 1.06\mu s$), and UNI ($\tau_d = 1.06\mu s$) mobile environments with number of turbo iterations set to five.

V. Conclusions

In this paper, we first study the effects of periodic termination of the state equation of a dynamic system. It is seen that periodic termination causes the trellis representation of the state equation to become a series of sub-trellises of much shorter length. This in turn enhances trajectory diversity and retards weight degeneracy. With these problems of traditional SMC frameworks mitigated, we then propose circumventing the resampling step, which allows us to achieve highly parallelized computation.

The non-resampling SMC framework is then applied to symbol detection in a coded OFDM system employing periodically terminated differential QPSK modulation. Simulation results are presented for convolutional and LDPC-coded systems and these results suggest the promising performance of the non-resampling SMC detector.

References

[1] L. J. Cimini, Jr., "Analysis and simulation of a digital mobile channel using orthogonal frequency division multiplexing," *IEEE Trans. Commun.*, vol. COM–33, pp. 665–675, July 1985.

[2] L. J. Cimini, Jr., B. Daneshrad, and N. R. Sollenberger, "Clustered OFDM with transmitter diversity and coding," in *Proc. 1996 IEEE Global Telecomm. Conf.*, Nov. 1996, pp. 703–707.

[3] I. Kalet, "The multitone channel," *IEEE Trans. Commun.*, vol. 37, pp. 119–124, Feb. 1989.

[4] S. B. Weinstein and P. M. Ebert, "Data transmission by frequency-division multiplexing using the discrete Fourier transform," *IEEE Trans. Commun.*, vol. COM–19, pp. 628–634, Oct. 1971.

[5] R. Chen and J. Liu, "Mixture Kalman filters," *J. R. Statist. Soc. B*, vol. 62, pp. 493–508, 2000.

[6] A. Doucet, S. J. Godsill, and C. Andrieu, "On sequential Monte Carlo sampling methods for Bayesian filtering," *Statist. Comput.*, vol. 10, no. 3, pp. 197–208, 2001.

[7] A. Kong, J. Liu, and W. Wong, "Sequential imputations and Bayesian missing data problems," *J. Amer. Statist. Assoc.*, vol. 89, pp. 278–288, 1994.

[8] M. Pitt and N. Shephard, "Filtering via simulation: Auxiliary particle filters," *J. Amer. Statist. Assoc.*, vol. 94, pp. 590–599, 1999.

[9] J. Liu and R. Chen,, "Sequential Monte Carlo methods for dynamic systems," *J. Amer. Statist. Assoc.*, vol. 93, pp. 1032–1044, 1998.

[10] — "Blind deconvolution via sequential imputations," *J. Amer. Statist. Assoc.*, vol. 90, pp. 567–576, 1995.

[11] R. Chen, X.Wang, and J. S. Liu, "Adaptive joint detection and decoding in flat-fading channels via mixture Kalman filtering," *IEEE Trans. Inform. Theory*, vol. 46, pp. 2079–2094, Sept. 2000.

[12] B. Dong, X. Wang, and A. Doucet, "A new class of soft MIMO demodulation algorithms," *IEEE Trans. Signal Processing*, vol. 50, pp. 2752–2763, Nov. 2003.

[13] Z. Yang and X. Wang, "A sequential Monte Carlo blind receiver for OFDM systems in frequency-selective fading channels," *IEEE Trans. Signal Processing*, vol. 50, pp. 271–280, Feb. 2002.

[14] M. Bolic, P. M. Djuric, and S. Hong, "New resampling algorithm for particle filters," in *Proc. IEEE of ICASSP*, Apr. 2003.

[15] J. H Kotecha and P. M. Djuric, "Gaussian particle filtering," *IEEE Trans. Signal Processing*, vol. 51, pp. 2592–2601, Oct. 2003.

[16] J. H Kotecha and P. M. Djuric, "Gaussian sum particle filtering," *IEEE Trans. Signal Processing*, vol. 51, pp. 2602–2612, Oct. 2003.

[17] Y. Li, N. Seshadri, and S. Ariyavisitakul, "Channel estimation for transmitter diversity in OFDM systems in mobile wireless channels," *IEEE J. Select. Areas Commun. Wireless Commun. Series*, vol. 17, pp. 461–471, Mar. 1999.

[18] J. Hagenauer, E. Offer, and L. Papke, "Iterative decoding of binary block and convolutional codes," *IEEE Trans. Inform. Theory*, vol. 42, pp. 429–445, Mar. 1996

[19] Lin and Costello, *Error Control Coding: Fundamentals and Applications.* Englewood Cliffs, NJ: Prentice–Hall, 1983.

[20] P. Hoeher, S. Kaiser, and P. Robertson, "Two-Dimensional Pilot-Symbol-Aided Channel Estimation by Wiener Filtering," in *Proc. IEEE ICASSP '97*, pp. 1845–1848, Apr. 1997.

[21] J. Proakis, *Digital Communications*, 4th ed. New York: McGraw-Hill, 2001.

[22] W. C. Jakes, Jr., *Microwave Mobile Communications.* Piscataway, NJ: IEEE, 1974.

[23] L. Bahl, J. Cocke, F. Jelinek, and J. Raviv, "Optimal decoding of linear codes for minimizing symbol error rate," *IEEE Trans. Inform. Theory*, vol. IT-20, pp. 284–287, Mar. 1974.

[24] T. J. Richardson and R. L. Urbanke, "Capacity of low density parity check codes under message passing decoding," *IEEE Trans. Inform. Theory*, vol. 47, pp. 599–618, Feb. 2001.

Thomas S. John (S'03) received the B.Eng. and M.Eng. in Electrical Engineering from the National University of Singapore, Singapore, in 2003 and 2005, respectively. Currently, he is pursuing his Ph.D. at Stanford University. His current research interests are statistical signal processing, OFDM and wireless communications theory.

Nallanathan Arumugam (S'97−M'00−SM'05) received the B.Sc. with honors from the University of Peradeniya, Sri-Lanka, in 1991, the CPGS from the University of Cambridge, United Kingdom, in 1994 and the Ph.D. from the University of Hong Kong, Hong Kong, in 2000, all in Electrical Engineering.

He was a Lecturer in the Department of Electrical and Electronic Engineering, University of Peradeniya, Sri-Lanka. Currently, he is an Assistant Professor in the Department of Electrical and Computer Engineering, National University of Singapore, Singapore. His current research interests are high-speed data transmission over wireless links, OFDM, ultra-wideband communications systems, and wireless communications theory.

Dr. Nallanathan is an Associate Editor for the EURASIP Journal on Wireless communications and Networking and a Guest Editor for EURASIP JWCN: Special issue on UWB Communication Systems-Technology and Applications.

Marc A. Armand (M'00) received the B.Eng. and Ph.D. in electrical engineering from the University of Bristol, Bristol, U.K., in 1995 and 1999, respectively.

Since 2000, he has been an Assistant Professor in the Department of Electrical and Computer Engineering at the National University of Singapore. His research interest include information theory and coding theory and techniques.